*Figure 1* (a) Electron diffraction pattern obtained from a deformed single crystal of polyoxymethylene. (b) Tracing of the electron diffraction pattern shown in (a). The reflections from the hexagonal and the two orthorhombic phases are represented by filled circles and open and filled triangles respectively. (c) and (d) are schematic diagrams of the hexagonal and orthorhombic lattices showing the orientation relationships between the two phases as represented by the electron diffraction pattern in (a). The unit cells are indicated by bold lines.

lattice parameters of the orthorhombic phase the previously reported lattice parameters of the hexagonal phase were used, $a = 4.46$ Å, and it was assumed that the lattice parameter $c$ remains invariant under the transformation at $c = 17.3$ Å.

The lattice parameters of the orthorhombic phase were calculated from the measurements of electron diffraction patterns of deformed polyoxymethylene single crystals to be $a = 4.96 \pm 0.03$ Å and $b = 7.44 \pm 0.04$ Å. Within experimental error these parameters are indistinguishable from those of polyethylene. No polyethylene was present, however, during the preparation of the crystals, and in such a case the familiar diamond shaped polyethylene crystals would have been detected. The orientation relationships observed are also quite different from those observed by Takahashi [10] in the polyethylene single crystals grown eptaxially on polyoxymethylene single crystals.

Many electron diffraction patterns of the type shown in Fig. 1a were recorded and show that a hexagonal to orthorhombic phase transformation in polyoxymethylene is operative under the conditions of test described. It is, therefore, possible that the same transformation process could be operative in cold-rolled polyoxymethylene as postulated by Preedy and Wheeler [1].

## Acknowledgements

The authors are indebted to the Science Research Council for financial support and to Mr P. Allan for valuable discussions. The authors are also indebted to Mr J. Preedy for suggesting that they and their co-workers should extend their studies of stress induced transformations and twinning in semi-crystalline polymers to include polyoxymethylene.

## References

1. J. E. PREEDY and E. J. WHEELER, *Nature, Phys. Sci.* **236** (1972) 60.
2. G. A. CARAZZOLO and M. MAMMI, *J. Polymer Sci.* **A1** (1963) 965.
3. H. TADOKORO, T. YASUMOTO, S. MURAHASHI and I. NITTA, *ibid* **44** (1960) 266.
4. E. H. ANDREWS and G. E. MARTIN, *J. Mater. Sci.* **8** (1973) 1315.
5. E. P. CHANG, R. W. GRAY and N. G. MCCRUM, *ibid* **8** (1973) 397.
6. T. SETO, T. HARA and K. TANAKA, *Jap. J. Appl. Phys.* **7** (1968) 31.
7. P. S. ALLAN, E. B. CRELLIN and M. BEVIS, *Phil. Mag.* **27** (1973) 127.
8. N. HARRIS and M. BEVIS, to be published.
9. K. J. O'LEARY and P. H. GEIL, *J. Macromol. Sci. Phys. B* **2** (1968) 261.
10. T. TAKAHASI, in "Encylcopaedia of Polymer Science and Technology" (Interscience Publishers, New York, 1968) Vol. 9, p. 239.

*Received 24 July*
*and accepted 29 July 1974*

N. HARRIS*
M. BEVIS
*Department of Metallurgy and Materials Science,*
*University of Liverpool, UK*

---

*Present address: University of London Careers Advisory Service, 50 Gordon Square, London, UK

---

## *The change in deviation parameter on crossing a phase or twin boundary*

It is well known that diffraction contrast in the electron image of a crystal is sensitively dependent upon the exact orientation relative to the electron beam [1]. When a phase or twin boundary is present in the field of view, oriented nearly parallel to the beam, a difference in diffraction conditions pertains on either side of the boundary, and corresponding differences in contrast occur. Examples have been discussed recently in papers dealing with molecular crystals [2, 3]. In both studies there are regions of interest in which significant departure from a Bragg orientation is present on either side of a boundary. In the "real space crystallography" analysis of Jones and Williams, they assume that their films have a constant curvature over the field of view and estimate local orientations at positions distant from the several bend contours observed in bright field [2]. The study of polyethylene in which twins were found employed sub-visual selection of areas for imaging, making orientation adjustments impossible, and resulting in matrix/twin pairs in which both have significant deviation parameters (denoted $s$, see [1]). It is hence of interest to know the change in $s$ across such a boundary under these conditions.

Let us choose a cartesian co-ordinate system with the $z$-axis in the direction of the electron beam, and the $y$-axis perpendicular to the plane defined by the electron beam and the diffraction vector, $\mathbf{g}_1$, corresponding to the first phase (matrix), see Fig. 1. Thus $\mathbf{g}_1$ lies in the $xz$-plane, and makes an angle $\theta$ (= the Bragg angle) with the $x$-axis when the crystal is Bragg oriented with respect to the corresponding family of planes. In the general case shown in Fig.1 the crystal is misoriented by a rotation $\gamma$ about the $y$-axis.

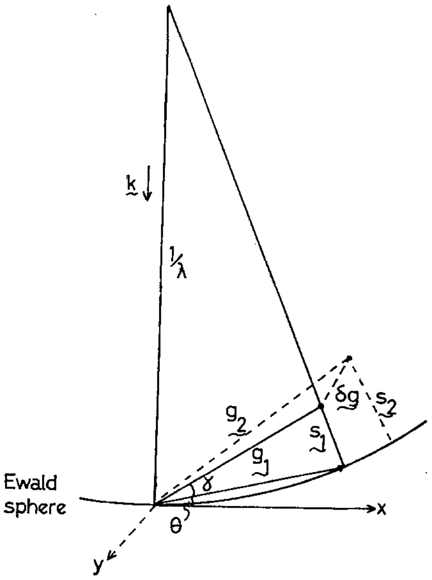

*Figure 1* Ewald sphere construction. $\mathbf{g}_2$, $\mathbf{s}_2$ and $\boldsymbol{\delta}\mathbf{g}$ are represented by broken lines to indicate they need not lie in the $xz$-plane. The reciprocal lattice vector which is shown terminating on the Ewald sphere is constructed in the position taken by $\mathbf{g}_1$ when the first crystal is Bragg-oriented for this reflection.

The origin is chosen as the position where the electron beam intersects the Ewald sphere. Hence if $\mathbf{i}$, $\mathbf{j}$ and $\mathbf{k}$ are unit vectors parallel to the $x$-, $y$-, and $z$-axes respectively we can write:

$$\mathbf{g}_1 = g_1 \cos(\gamma + \theta)\mathbf{i} - g_1 \sin(\gamma + \theta)\mathbf{k}\,.$$

The deviation parameters shown in Fig. 1 have been chosen to lie along radii of the Ewald sphere for convenience of calculation. It can easily be shown that this approximation is extremely accurate for most cases met in practice. Hence if the radius of the Ewald sphere is $1/\lambda$ (where $\lambda$ is the electron wavelength) the magnitude of the deviation parameter, $s_1$, corresponding to $\mathbf{g}_1$ is

$$s_1 = \frac{1}{\lambda} - \left|\frac{1}{\lambda}\mathbf{k} + \mathbf{g}_1\right| = \frac{1}{\lambda}$$
$$- \frac{1}{\lambda}\,[1 + (\lambda^2 g_1{}^2) + (2\lambda \mathbf{g}_1 . \mathbf{k})]^{\frac{1}{2}}$$

The second phase (twin) diffraction vector of interest will generally be the one terminating nearest to the terminal point of $\mathbf{g}_1$ and is denoted by $\mathbf{g}_2$. $\mathbf{g}_2$ and the corresponding deviation parameter $\mathbf{s}_2$ do not necessarily lie in the $xz$-plane.

If $\mathbf{g}_1 + \boldsymbol{\delta}\mathbf{g} = \mathbf{g}_2$

then

$$s_2 = \frac{1}{\lambda} - \left|\frac{1}{\lambda}\mathbf{k} + \mathbf{g}_1 + \boldsymbol{\delta}\mathbf{g}\right|$$

$$= \frac{1}{\lambda} - \frac{1}{\lambda}\,\{1 + [\lambda^2 g_1{}^2] + [2\lambda \mathbf{g}_1 . \mathbf{k}] + [\lambda^2(\delta g)^2]$$
$$+ [2\lambda \boldsymbol{\delta}\mathbf{g} . \mathbf{k}] + [2\lambda^2 \mathbf{g}_1 . \boldsymbol{\delta}\mathbf{g}]\}^{\frac{1}{2}}$$

$\lambda g_1 \ll 1$ and $\lambda \delta g \ll 1$.

Thus, using the binomial expansion:

$$s_1 = -\left(\frac{\lambda g_1{}^2}{2} + \mathbf{g}_1 . \mathbf{k}\right)$$

and

$$s_2 = -\left\{\frac{\lambda g_1{}^2}{2} + \mathbf{g}_1 . \mathbf{k} + \frac{\lambda(\delta g)^2}{2}\right.$$
$$\left. + \boldsymbol{\delta}\mathbf{g} . \mathbf{k} + \lambda \mathbf{g}_1 . \boldsymbol{\delta}\mathbf{g}\right\}$$

$$s_1 - s_2 = \delta s$$
$$= \left\{[\lambda \mathbf{g}_1 . \boldsymbol{\delta}\mathbf{g}] + [\boldsymbol{\delta}\mathbf{g} . \mathbf{k}] + \left[\frac{\lambda(\delta g)^2}{2}\right]\right\}.$$

If $\lambda$ is replaced by $2\theta/g_1$ (Bragg's law),

$$\delta s = \frac{2\theta \mathbf{g}_1 . \boldsymbol{\delta}\mathbf{g}}{g_1} + \boldsymbol{\delta}\mathbf{g} . \mathbf{k} + \frac{\lambda(\delta g)^2}{2}\,. \qquad (1)$$

Consider now the case where $\boldsymbol{\delta}\mathbf{g} \parallel \mathbf{g}_1$ (cf. Fig. D3 of [4]), then

$$\delta\mathbf{g} \cdot \mathbf{k} \equiv \frac{\mathbf{g}_1 \cdot \mathbf{k}}{g_1}\,\delta g = \frac{\mathbf{g}_1 \cdot \mathbf{k}}{g_1}\,\frac{\mathbf{g}_1 \cdot \delta\mathbf{g}}{g_1}$$

$$= -\sin(\gamma + \theta)\,\frac{\mathbf{g}_1 \cdot \delta\mathbf{g}}{g_1}$$

$$= -(\gamma + \theta)\,\frac{\mathbf{g}_1 \cdot \delta\mathbf{g}}{g_1}$$

$$\delta s = \{2\theta - (\gamma + \theta)\}\,\frac{\mathbf{g}_1 \cdot \delta\mathbf{g}}{g_1} + \frac{\lambda(\delta g)^2}{2}$$

$$= (\theta - \gamma)\,\frac{\mathbf{g}_1 \cdot \delta\mathbf{g}}{g_1} + \frac{\lambda(\delta g)^2}{2}\,.$$

If $\delta g$ is small, this reduces to

$$\delta s = (\theta - \gamma)\,\frac{\mathbf{g}_1 \cdot \delta\mathbf{g}}{g_1}\,. \qquad (2)$$

The expression given by Goringe and Valdrè is obtained from Equation 2 by setting $\gamma = 0$, and is hence valid only when $\theta \gg \gamma$. This condition is often violated in practice, as for example in the studies of Jones and Williams [2] and of White [3] and the $\gamma$-dependent term can become dominant. The simple version found in [4] can, therefore, only be applied to special situations and the general form given above as Equation 1 must normally be employed.

## Acknowledgements

I am grateful to Drs Jones and Williams for a copy of their manuscript prior to publication, and to the Science Research Council for financial support.

## References

1. P. B. HIRSCH, A. HOWIE, R. B. NICHOLSON, D. W. PASHLEY and M. J. WHELAN, "Electron Microscopy of Thin Crystals" (Butterworths, London, 1965).
2. W. JONES and J. O. WILLIAMS, *J. Mater. Sci.* **10** (1975) 379.
3. J. R. WHITE, *ibid* **9** (1974) 1860.
4. M. J. GORINGE and U. VALDRÈ, *Proc. Roy. Soc.* **A295** (1966) 192.

*Received 11 October*
*and accepted 24 October 1974*

J. R. WHITE
*Department of Materials,*
*Queen Mary College,*
*London, UK*

---

## *A TEM study of precipitates in Cu$_2$O*

The microscopic precipitate structure of cuprous oxide $Cu_2O$ prepared either by total oxidation of copper or by growth from the melt has recently been investigated [1]. Those precipitates visible in the optical microscope are agglomerates of cupric oxide CuO formed during cooling from the elevated temperatures of crystal growth.

The work reported in this note was undertaken in order to investigate the efficiency, on a submicroscopic scale, of the annealing treatment designed to eliminate such agglomerates [1].

Single crystals were prepared from copper of two purities (99.9 and 99.999%) by total oxidation and growth by a floating zone method. Slices 0.2 mm thick were cut from annealed specimens and chemically tailored in concentrated nitric acid to form 3 mm diameter discs. These discs were polished chemically in a solution of 90% orthophosphoric acid and 10% nitric acid [2] in a double jet Tenupol apparatus until the central portion assumed a yellow colour indicating a thickness of about 1000 Å [3]. Thinning was continued either by ion bombardment (6 keV Ar ions), or chemically by immersion first in a bath of 80% orthophosphoric acid and 10% nitric acid for several minutes, and then in a solution of 80% orthophosphoric acid and 5% nitric acid until a hole was formed.

Thinned specimens were examined in a Philips EM300 electron microscope operating at 100 kV with hot stage and tilting accessories.*

At the beginning of the TEM observation, thin foils obtained by ion bombardment showed no trace of a second phase even at the limit of resolution. In chemically thinned specimens, large facetted deposits impervious to electrons were observed on the surface of the otherwise precipitate-free foils. After an observation time of typically 20 to 30 min with a low intensity electron beam, disc-shaped inclusions of 50 to 200 Å diameter developed both in foils thinned chemically and by ion bombardment (Fig. 1). Selected-area diffraction revealed the presence of

*C.E.C.M., Vitry sur Seine.